ELSEVIER

Physica C 308 (1998) 301–311

PHYSICA C

Exact-diagonalization study on the effect of the long-range Coulomb interaction to the superconducting ground state in the two-chain Hubbard model

Soh Koike [a,b,*], Kunihiko Yamaji [b,a], Takashi Yanagisawa [b]

[a] *Institute of Materials Science, University of Tsukuba, 1-1-1 Ten-nodai, Tsukuba, Ibaraki, 305-8573, Japan*
[b] *Electrotechnical Laboratory, 1-1-4 Umezono, Tsukuba, Ibaraki, 305-8568, Japan*

Received 4 August 1998; revised 20 August 1998; accepted 17 September 1998

Abstract

We present exact-diagonalization results clearly indicating that the long-range part of Coulomb interaction does not sweep away the superconducting region of the two-chain Hubbard model driven by the short-range part. When the model contains the nearest-neighbor Coulomb interaction both for the interchain and the intrachain directions, the region of developed superconducting correlations in the ground state is reduced. The CDW correlation is found to increase, intervening with the competition between superconductivity and CDW. When we include the long-range Coulomb interaction of the type of $1/r$, the instability to the CDW state weakens with the superconducting region recovered to some extent compared with the above case.

PACS: 74.20.Mn; 74.70.-b; 71.10.Hf; 71.45.Lr

Keywords: Superconductivity; Two-chain Hubbard model; Long-range Coulomb interaction; CDW; Exact-diagonalization method

1. Introduction

The two-chain (2C) Hubbard model is the simplest and most basic one which is possibly able to exhibit superconductivity due to the Coulomb interaction. This model can be rewritten into a two-band model consisting of bonding and antibonding bands [1]. Exact-diagonalization studies of the 2C Hubbard model were carried out to examine the possibility that the superconductivity occurs in this model driven by the transfer process [2] of the electron pairs between the two bands, which is generated by the on-site Coulomb interaction [1,3,4]. In a wide parameter region of the model the occurrence of the superconductivity was strongly indicated. The superconducting (SC) features were most enhanced when the Fermi energy lies near the bottom of the upper-side band in this calculation [3].

The bosonization method was employed to investigate the ground state properties of this model [5–8].

* Corresponding author. Telefax: +81-298-54-5099; E-mail: eveso@etl.go.jp

0921-4534/98/$19.00
PII: S0921-4534(98)00529-2

It was found that there is a parameter region where there is a finite gap for spin excitations but no gap for charge excitations. In this region the so-called duality relation, $K_{SC} \cdot K_{CDW} = 1$, was found where K_{SC} is the exponent for the SC correlation function and K_{CDW} is that for the $4k_F$-CDW correlation; the latter is that for the $4k_F$ charge density wave along a chain; here $4k_F$ is the $4k_F$ wave number along a chain, which is equal to 2π times electron density per site. This relation was first found in the case where the interchain electron-transfer energy t_d is quite small so that the coupling constant for the backward scattering, produced by the effect of the finite t_d between the two chains, can be treated as a perturbation. The SC state dominates when $K_{SC} < 1$. The duality relation means that the SC state competes with the $4k_F$-CDW state. When t_d is not so small, the bosonization method loses its power for analysis due to the intricateness of its phase Hamiltonian. In order to avoid this difficulty, the multiplicative renormalization group technique for all kinds of coupling constants [9–13] was employed together with the bosonization method. The existence of the spin gap was observed widely in such a parameter region where the Fermi level crosses both the bonding and the antibonding bands in the 2C Hubbard model, and that the above duality relation was also satisfied in this spin gap region [14–16]. It is difficult to clarify the correlation of which ordering is dominant in the spin gap region in the 2C Hubbard model analytically in general. However, in the case where the Fermi velocity in the bonding band is equal to that in the antibonding band, the K_{SC} is nearly equal to $1/2$ in the weak coupling limit. According to the result of Balents and Fisher [16], the larger the value of the Fermi velocity in the bonding band compared with that in the antibonding one, the more stable the SC state. Therefore, the superconductivity should occur in this model. However these results are valid only in the weak coupling cases.

The 2C Hubbard model was also studied numerically in the intermediate and strong coupling regions [17–20]. Noack et. al. [17], calculated the SC correlation function and $4k_F$-CDW correlation function for this model of considerable sizes in the case of the electron density equal to 0.875 and on-site Coulomb energy $U_0 = 8t$, where t is the transfer energy between the nearest-neighbor (n.n.) sites along the chain, using the density matrix renormalization group method [21,22]. They displayed that both correlation functions decay holding a power law as a function of the distance and the SC correlation is dominant in a region of t_d around $1.5t$. However, the above-mentioned duality relation did not seem to be satisfied in their result. We studied the size-dependence of the energy difference per site between the SC state and the normal state by use of the variational Monte Carlo method in the case of the electron-density equal to 0.833, $t_d = 1.5t$ and $U_0 = 8t$ on the lattice with up to 72×2 sites [22]. We obtained a scaling law for the energy gain per site in the SC state with respect to the system size and confirmed that the energy gain per site remains finite in the bulk limit. Therefore it is almost established that the superconductivity occurs in a certain parameter region in the 2C Hubbard model.

There are some materials such as $Ni(dmit)_2$ compounds [23] and $Sr_{14-x}Ca_xCu_{24}O_{41}$ [24] which have a two-leg ladder in their crystal structures and exhibit SC characters. There is a possibility that the superconductivity in these materials occurs due to the ladder part basically substantiating the 2C Hubbard model. The ladder part of those materials can be approximately modeled into the 2C Hubbard model.

However, the long-range part of the Coulomb interaction in the real materials is dropped out in this model. In applying this model to real materials, taking account of this dropped part may bring about serious effects. Especially, the n.n. interchain Coulomb interaction with coupling constant V_d was considered to work negatively against the superconductivity. Because of this term, the coupling constant for the intraband Coulomb scattering enlarges, and that for the interband electron-pair transfer reduces. Both effects should oppose to the occurrence of superconductivity in this system. In a previous work [25] we investigated the effect of this interaction with coupling constant V_d to the superconductivity by use of the exact diagonalization and found that the SC region survives tenaciously in a wide parameter region in spite of detrimental effects of the interaction. In this paper we have investigated the effect of other types of the long-range Coulomb interaction, i.e., n.n. intrachain Coulomb interaction, n.n. Coulomb interaction with both interchain and

intrachain parts, and the long-range Coulomb interaction of the type of $1/r$ by use of the exact-diagonalization method and have confirmed the above-mentioned viability of the superconductivity against the realistic long-range Coulomb interaction. We have also paid attention to the competing CDW correlation.

In Section 2, the model is introduced and the effect of the n.n. intrachain Coulomb interaction, the n.n. Coulomb interaction for both intrachain and interchain directions are examined. In Section 3, we treat the long-range Coulomb interaction of the $1/r$ type in the 2C Hubbard model and summarize results in Section 4.

2. Model and results

2.1. Model and superconducting correlation functions

The Hamiltonian containing the n.n. interchain and intrachain Coulomb interactions is defined as

$$H = H_0 + H_1 + H_2, \tag{1}$$

$$H_0 = -t_d \sum_{l,\sigma} \left(c^{\dagger}_{1l\sigma} c_{2l\sigma} + \text{H.c.} \right) - t \sum_{j=1}^{2} \sum_{l,\sigma} \left(c^{\dagger}_{jl\sigma} c_{j,l+1,\sigma} + \text{H.c.} \right), \tag{2}$$

$$H_1 = U_0 \sum_{j=1}^{2} \sum_{l} c^{\dagger}_{jl\uparrow} c_{jl\uparrow} c^{\dagger}_{jl\downarrow} c_{jl\downarrow}, \tag{3}$$

$$H_2 = V_d \sum_{l,\sigma,\sigma'} c^{\dagger}_{1l\sigma} c_{1l\sigma} c^{\dagger}_{2l\sigma'} c_{2l\sigma'} + V_p \sum_{j=1}^{2} \sum_{l\sigma\sigma'} c^{\dagger}_{jl\sigma} c_{jl\sigma} c^{\dagger}_{j,l+1,\sigma'} c_{j,l+1,\sigma'}, \tag{4}$$

where t (t_d) is the intrachain (interchain) transfer energy, H.c. means the Hermite conjugate term, H_1 is the Coulomb interaction with on-site Coulomb energy U_0, and H_2 consists of the n.n. interchain Coulomb interaction with coupling constant V_d and the n.n. intrachain one with coupling constant V_p, and $c_{jl\sigma}$ ($c^{\dagger}_{jl\sigma}$) is the annihilation (creation) operator of an electron with spin σ at the lth site along the jth chain ($j = 1,2$). The schematic figure of the model is shown in Fig. 1. The H_0 part can be diagonalized by making Fourier transformation

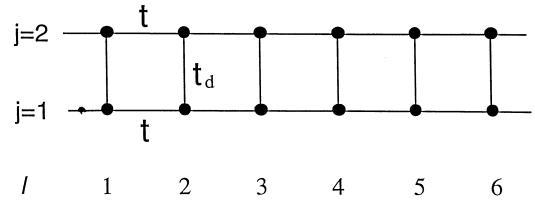

Fig. 1. The schematic figure of the 2C Hubbard model. Closed circles are the electronic sites.

$$a_{k\sigma} = \sum_{jl} c_{jl\sigma} e^{i(k_x l + k_y (j-1))} / \sqrt{2N}, \tag{5}$$

where N is the number of rungs; $k_y = 0$ or π, which corresponds to the bonding and the antibonding band, respectively, given as $\varepsilon_k = -2t\cos k_x - t_d \cos k_y$. Throughout this paper we employ the antiperiodic boundary condition along the chain so that the system has an open shell structure with ten electrons. Consequently $k_x = (2\upsilon + 1)\pi/N$ ($\upsilon = 0,1,\cdots, N-1$).

2.2. Effect of the intrachain nearest-neighbor Coulomb coupling

In the previous work, we found that the n.n. interchain Coulomb interaction, i.e., with finite V_d and vanishing V_p, destroys the SC phase only moderately [25]. This was considered to be due to the fact that V_d enlarges the antiferromagnetic coupling in the rung, compensating the effect of separating the pair of electrons on the rung by its repulsive force. However, with the intention of applying the results for the 2C Hubbard model to real materials, we have to include more general forms of long-range interactions into the 2C Hubbard model. First, we examine the effect of the n.n. intrachain Coulomb interaction without the n.n. interchain interaction part. The Hamiltonian is given by Eq. (1) with finite V_p and $V_d = 0$ in Eq. (4). We investigate the ground state

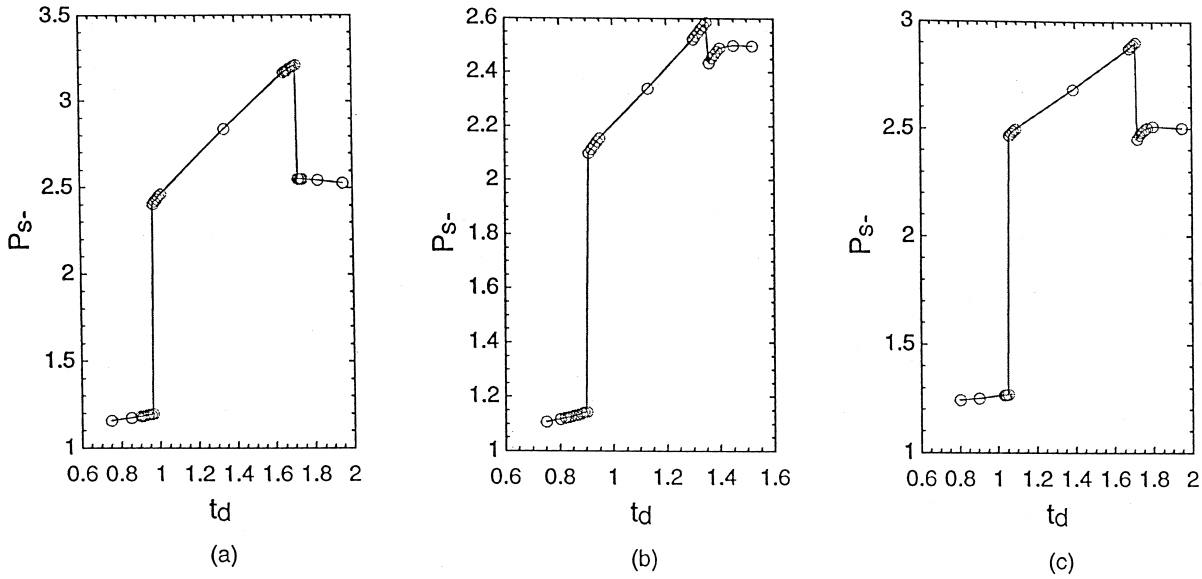

Fig. 2. The behavior of the SC pair correlation function $P_{s\_}$ as a function of t_d are shown in some cases. The value of the on-site Coulomb interaction U_0 is equal to 8. (a) is for the case of $V_d = V_p = 0$. (b) the case of $V_d = 2$, $V_p = 0$. (c) the case of $V_d = 0$, $V_p = 2$.

properties of this model using the exact-diagonalization method similarly as in the previous work. The system we treat is a ladder with six rungs and two legs having ten electrons. We fix the value of on-site Coulomb energy U_0 at $8t$. Hereafter we take t as the energy unit.

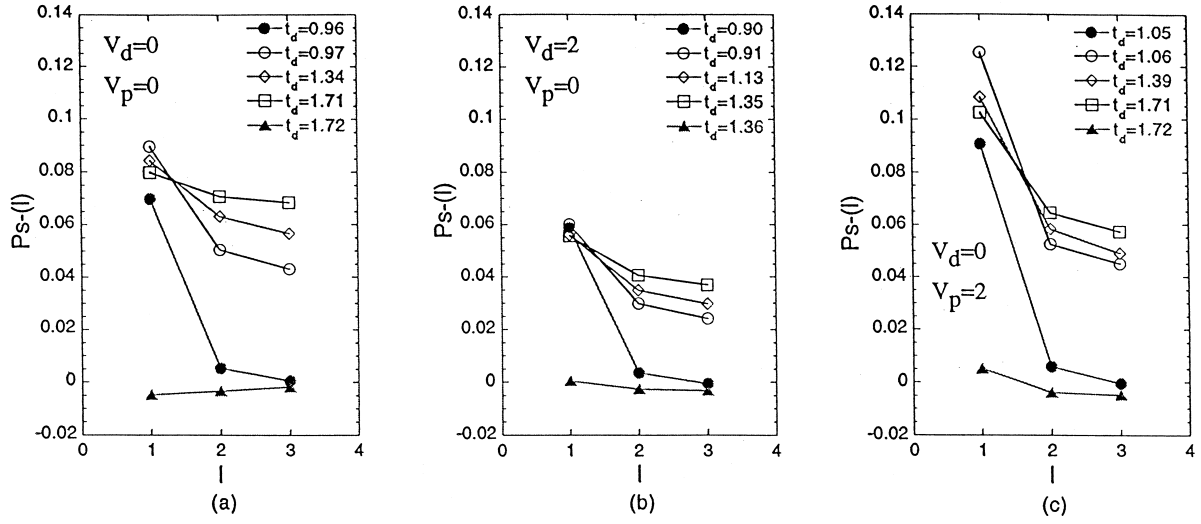

Fig. 3. The behavior of SC pair correlation function $P_{s\_}(m)$ as a function of distance m between pairs is shown in some cases. The value of on-site Coulomb interaction U_0 is equal to 8. (a) is for the case of $V_d = V_p = 0$. (b) the case of $V_d = 2$, $V_p = 0$. (c) the case of $V_d = 0$, $V_p = 2$. When we introduce the n.n. intrachain Coulomb interaction V_p in the model, $P_{s\_}(m)$ as a function of m decays more quickly.

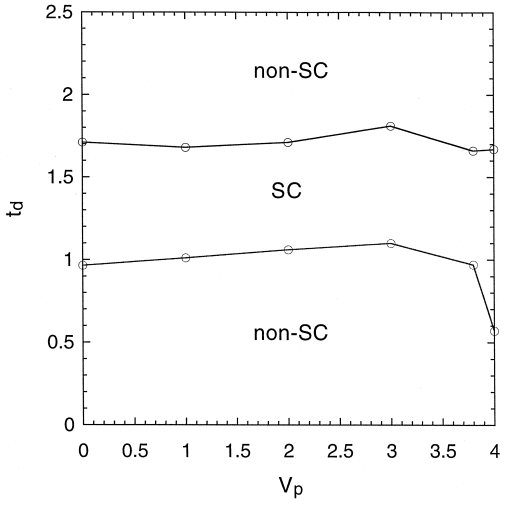

Fig. 4. The SC phase diagram of the 2C Hubbard model including the n.n. intrachain Coulomb interaction V_p. The energy unit is t which is the intrachain transfer energy of electron. The value of the on-site Coulomb energy U_0 is equal to 8. The region of the SC phase is not significantly diminished by the introduction of finite V_p.

We obtain the ground state wave function $|g\rangle$ and calculate the following SC pair correlation functions from which we judge the nature of the ground state:

$$P_{s-} = \langle g|\Delta_-^\dagger \Delta_- + \text{H.c.}|g\rangle, \tag{6}$$

$$P_{s-}(m) = \sum_l \langle g|\Delta_-^\dagger(l)\,\Delta_-(l+m)|g\rangle/N, \tag{7}$$

where the pair operators are defined by

$$\Delta_- = \sum_l \Delta_-(l)/\sqrt{N}, \tag{8}$$

$$\Delta_-(l) = c_{1l\downarrow}c_{2l\uparrow} - c_{1l\uparrow}c_{2l\downarrow}. \tag{9}$$

$\Delta_-(l)$ is the operator annihilating the singlet pair on the lth rung.

When we varied t_d, there was a parameter region where the value of P_{s-} was enhanced, forming a plateau as in Fig. 2, and at the same time the decay rate of $P_{s-}(m)$ with increase of distance m was much smaller than in other regions, as shown in Fig. 3. These features strongly indicated the occurrence of the superconductivity in this parameter region [1,3]. We interpret that in this region the system is in an SC state and call such a region SC region, as in the previous papers.

The obtained SC region as a function of U_0 and t_d is shown in Fig. 4. As shown in this figure, the SC region does not diminish significantly even when V_p is finite in contrast with the case of V_d [25]. Therefore, the detrimental effect of V_p to superconductivity is apparently more moderate than that of V_d. When $V_p \gtrsim 4(=U_0/2)$, the region indicating superconductivity enlarges; here the effective on-site intercation is attractive since $2V_p \gtrsim U_0$ when the electron density $\rho \sim 1$. This aspect of V_p is considered to help the SC state survive against increasing V_p.

Another expectation of the effects of V_p is seen in the SC pair correlation function $P_{s-}(m)$ as a function of m between pairs; it is observed to decay slightly more quickly when V_p is non-zero, than in the case where $V_p = 0$. This is interpreted as due to the effect of V_p in the following way. When V_p increases, the electrons on the ladder are consider to

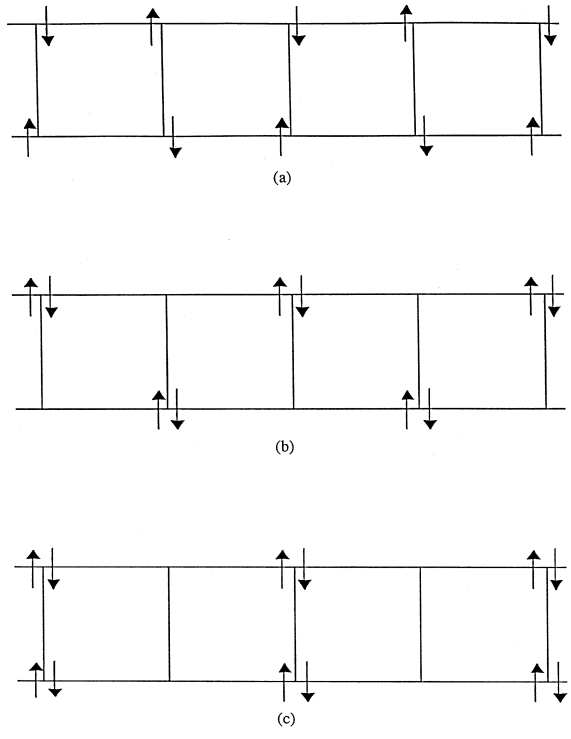

Fig. 5. (a) shows the state in which pairs of electrons form a singlet state on a rung. (b),(c) the state in which electrons form the CDW along the chain. When we introduce the n.n. intrachain Coulomb interaction V_p, the CDW correlation corresponding to the configuration like (b) or (c) increases.

tend to avoid the nearest neighbor sites each other along the chain and to occupy a site pair-wise, taking a configuration like Fig. 5(b) or (c). This is because when V_p increases and tends to satisfy $U_0 - 2V_p < 0$ the patterns in Fig. 5(b) and (c) tend to be more stablized than the uniform charge distribution. This corresponds to the formation of the CDW state. Even when $U_0 - 2V_p > 0$, the correlation of this CDW is considered to be enhanced. In competition with the CDW correlation the correlation of the singlet pairs on the rung is considered to be forced to decay slightly more quickly. When $U_0 - 2V_p < 0$ the SC correlation is seen to clearly win the competition.

In order to confirm this reasoning, we calculate the following CDW correlation function;

$$D(q_x,q_y) = \frac{1}{N}\sum_{j,j',l,l'} \langle g|n_{jl\uparrow}\, n_{jl\downarrow}\, n_{j'l'\uparrow}\, n_{j'l'\downarrow}|g\rangle \times \cos\big(q_x(l-l')\big)\cos\big(q_y(j-j')\big). \quad (10)$$

The obtained data of $D(q_x, q_y)$ is displayed in Fig. 6(a) with $t_d = 1.05$ for various value of V_p. The horizonal axis is q_x. Open (closed) symbols in the figure correspond to $q_y = 0(\pi)$. In our system, the number of electrons (N_e) is smaller than that of sites so the value of $D(q_x,q_y)$ should have the maximum at $q_x = \pi N_e/(2N) = 5\pi/6$ which is slightly less than π. However, the maximum value of $D(q_x,q_y)$ was found at $q_x = \pi$ in almost all the cases. This may be due to the smallness of the size of our system. The value of each component of $D(q_x,q_y)$ grows up when the n.n. intrachain repulsive Coulomb interaction V_p is increased. Thus we find that the CDW correlations are developed when V_p is introduced in the Hamiltonian. The result of calculated $D(q_x,q_y)$ in the case where H_2 contains only the n.n. interchain Coulomb interaction V_d is also shown in Fig. 6(b) where the coupling constant is equal to 2.5. Increase of each component of $D(q_x,q_y)$ with increase of V_p is much pronounced than with increase of V_d. We have also calculated the following correlation function D':

$$D' = D(\pi,\pi) - D(\pi,0). \quad (11)$$

The first term on the right-hand side of Eq. (11) increases when the correlation corresponding to the configuration in Fig. 5(b) develops and the second term does so when the correlation corresponding to Fig. 5(c). The values of D' are shown in Fig. 7(a) as

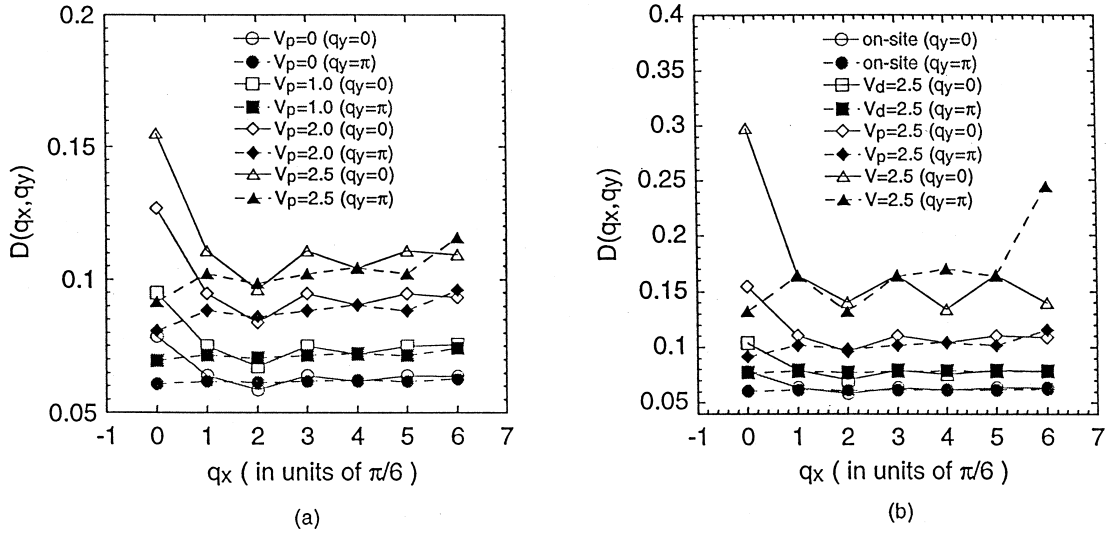

Fig. 6. ***q***-dependence of the CDW correlation function $D(q_x, q_y)$ in the case of $U_0 = 8$ and $t_d = 1.05$. Open (closed) symbols correspond to $q_y = 0(\pi)$. (a) Results for the case of the n.n. intrachain Coulomb interaction with coupling constant V_p. Circles, squares, diamonds and triangles correspond to V_p values 0, 1.0, 2.0 and 2.5, respectively. (b) Values of $D(q_x, q_y)$ for the various types of interaction. Circles correspond to the simple 2C Hubbard model, diamonds to the case with $V_d = 2.5$, squares to the case with $V_p = 2.5$ and triangles to the case with $V = 2.5$.

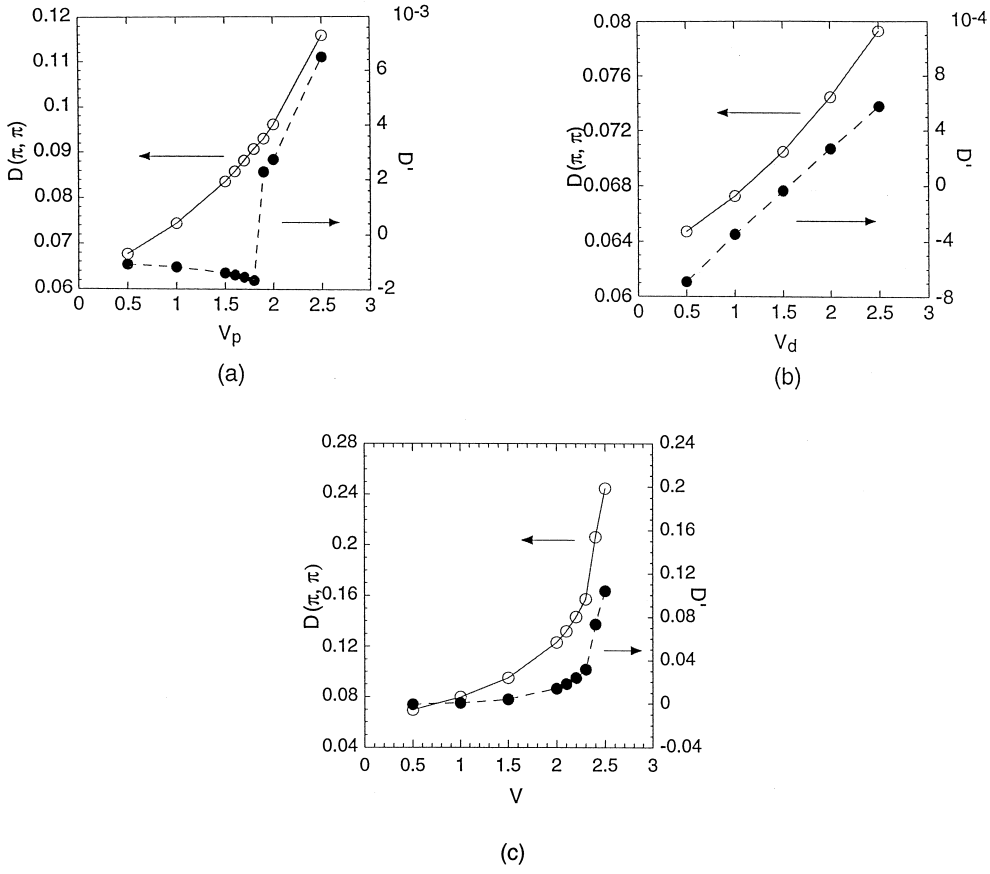

Fig. 7. The behavior of the CDW correlation function in each model in the case of $U_0 = 8$, $t_d = 1.05$. Open circles correspond to the value of $D(\pi, \pi)$ and closed circles to D'. (a) Results for the case of the n.n. intrachain Coulomb interaction with coupling constant V_p. (b) Results for the case of the n.n. interchain Coulomb interaction with coupling constant V_d. (c) Results for the case of the interchain and intrachain Coulomb interaction with coupling constant V.

a function of V_p with $V_d = 0$ and in Fig. 7(b) as a function of V_d with $V_p = 0$. We see that the value of D' has a small jump-wise enhancement at $V_p = 1.9$. This is just the point beyond which the SC correlation decreases in the case of $t_d = 1.05$. The small jump-wise enhancement is due to both a small downward jump of $D(\pi,0)$ and a gradual increase of $D(\pi,\pi)$.

These results indicate that V_p has a stronger effect for developing CDW correlations corresponding to the configuration like Fig. 5(b) and (c) in this system than V_d. In view of the duality relation, this is considered to cause the above-mentioned faster decay of $P_{s-}(m)$ as a function of m. However, it does not seem to narrow the SC region according to our result.

2.3. Effect of the intrachain and interchain n.n. Coulomb interaction

Next we consider the 2C Hubbard model including both the interchain and the intrachain n.n. Coulomb interactions with coupling constants $V_d = V_p = V$ in Eq. (4). According to our previous work, the region of the SC phase reduces only mildly by the introduction of the n.n. interchain Coulomb interaction with V_d. In the previous section we have found that it does more moderately by the action of

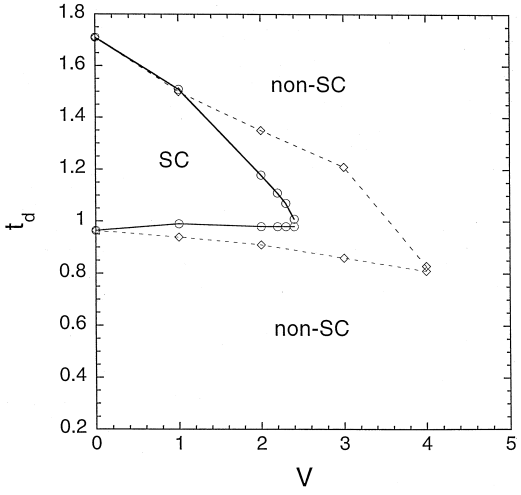

Fig. 8. The SC phase diagram of the 2C Hubbard model with the n.n. interchain and intrachain Coulomb interaction V. The broken curve is the SC phase diagram of the 2C Hubbard model with n.n. interchain Coulomb interaction with V_d; the value of V_d is equal to V. U_0 is equal to 8.

the n.n. intrachain Coulomb interaction V_p. Therefore, we expected that the SC phase diagram for the present model would be similar to that in the 2C Hubbard model including the n.n. interchain Coulomb interaction V_d.

We have calculated the correlation functions in the ground state under the same boundary condition with various values of V. The obtained SC phase diagram is shown in Fig. 8. The SC region decreased more rapidly with increasing V than in the case where we introduce the n.n. interchain Coulomb interaction V_d alone. We consider that it is because the electrons on the ladder are very much promoted to have a configuration in Fig. 5(b) due to both the n.n. intrachain and interchain Coulomb interaction V so that the instability to the CDW state becomes stronger with the features of the SC state weakening more rapidly.

In order to verify this reasoning, we calculate the value of $D(q_x,q_y)$ and D' defined in Eqs. (10) and (11), respectively, with $t_d = 1.05$ for various value of V. Results are shown in Figs. 6(b) and 7(c). As shown in Fig. 6(b), the CDW correlation develops more rapidly when the n.n. Coulomb interaction V for both the interchain and intrachain directions is introduced, than when either the n.n. interchain Coulomb interaction V_d or the n.n. intrachain one V_p alone is operative in the system. Both $D(\pi,0)$ and $D(\pi,\pi)$ showed jump-wise enhancement around $V = 2.4$ where the SC phase vanished. These jump-wise enhancement of $D(\pi,0)$ and $D(\pi,\pi)$ suggests the phase transition from the SC state to the CDW state. The value of the jump-wise enhancement of $D(\pi,\pi)$ between $V = 2.3$ and $V = 2.4$ is about 6.5 times larger than that of $D(\pi,0)$. Therefore, D' shows a jump-wise enhancement with a large value at $V = 2.4$ as is shown in Fig. 7(c). The configuration shown in Fig. 5(b) is preferred to that like Fig. 5(c) judging from the development of D'. This feature is similar but more prominent than in the case where the system has the n.n. intrachain Coulomb interaction with V_p alone. Apparently, the SC region in this system is replaced by the CDW-dominant region in a wider parameter region due to the prominent development of the CDW correlation competing with the SC correlation.

Here we add remarks on the effect of the boundary condition and the size effect. With ten electrons on the six-rung two-leg ladder we have an open shell situation in the most cases with the band parameters lying in the neighborhood of the phase boundary, i.e., some ***k***-points in the band are only partially

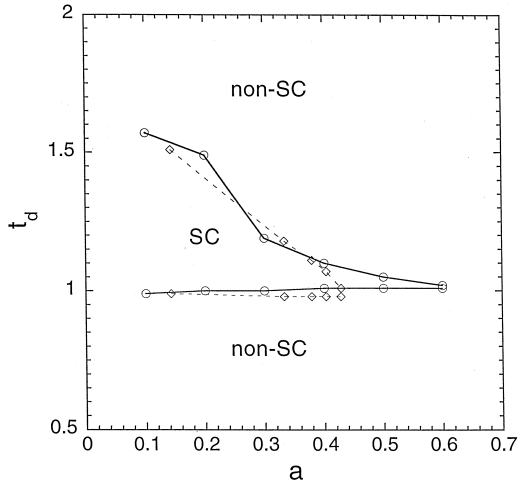

Fig. 9. The SC phase diagram of 2C Hubbard model including the Nishimoto–Mataga potential with $U_0 = 8$. The broken curve displays the phase boundary in the case where the interaction part for $r > 1$ is dropped, i.e., the case of the interchain and intrachain n.n. Coulomb interaction.

filled in the limit of $U_0 = 0$. In this situation P_{s-} is observed to increase jump-wise when the parameter set gets into the SC region. In the case of the closed shell with the periodic boundary condition, the transition between the two regions where the SC correlation is well developed and not so, respectively, is observed to be gradual. Therefore, it is difficult to define a clear-cut boundary. This is the reason why we employ the antiperiodic boundary condition in this work. This means that the thus obtained boundary is somewhat conventional. However, we consider that it works in a qualitative sense. Concerning the size effect, we agree that it is considerable and that all results are qualitative. However, we believe that obtained results show qualitatively corrected properties. Although the previous work [1] treated a system of small size, the results were later found to be qualitatively consistent with those of larger sizes [19–22]. This strongly suggests that the results obtained by the exact-diagonalization method for a ladder with six rungs and two legs having ten electrons are qualitatively valid, even though the size effect is considerable.

3. Two-chain Hubbard model including the long-range Coulomb interaction

Next we consider the 2C Hubbard model which is added with a long-range Coulomb interaction of the type of $1/r$. This model is closer to real materials than the previous ones. We want to examine if the further long-range part of the Coulomb interaction adds further detrimental effects or not. The interaction part of the Hamiltonian we consider here, i.e., $H_1 + H_2$ part in Eq. (1), is defined as

$$H_1 + H_2 = \frac{1}{2} \sum_{j,j',l,l',\sigma,\sigma'} V(r)\, c^{\dagger}_{jl\sigma} c_{jl\sigma} c^{\dagger}_{j'l'\sigma'} c_{j'l'\sigma'}, \tag{12}$$

where $V(r)$ is the Nishimoto–Mataga potential,

$$V(r) = \frac{U_0 a}{a + r}, \tag{13}$$

with $r = \sqrt{(j'-j)^2 + (l'-l)^2}$; a is a parameter decided by experiment in each material. We have obtained the SC region of the 2C Hubbard model

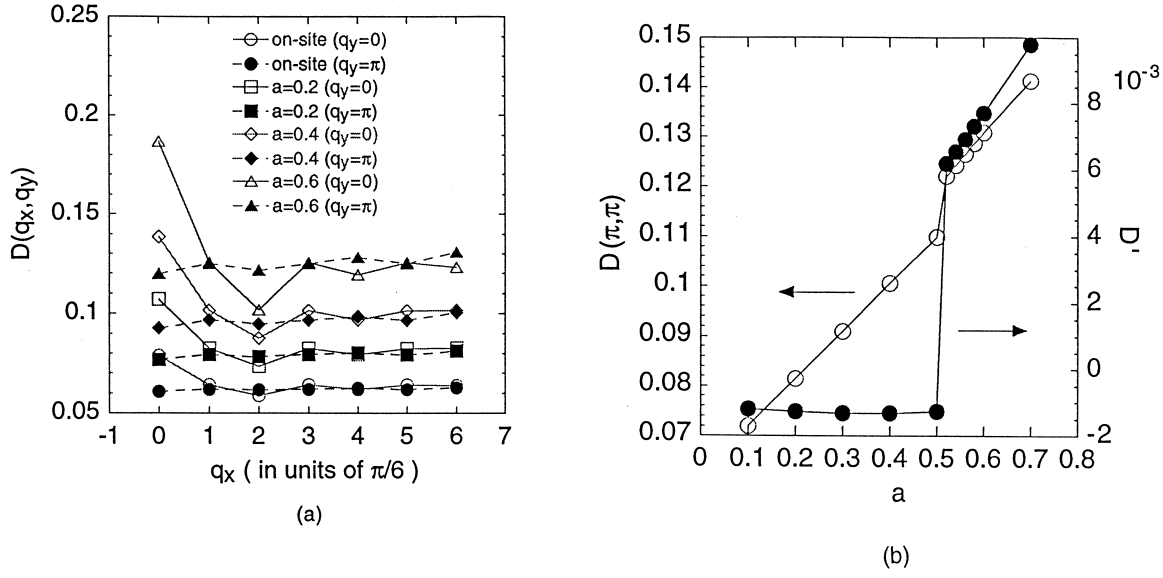

Fig. 10. The behavior of the CDW correlation function for the Nishimoto–Mataga potential in the case of $U_0 = 8$, $t_d = 1.05$. (a) Values of $D(q_x, q_y)$ for various a. Circles correspond to the simple 2C Hubbard model. Squares, diamonds and triangles correspond to $a = 0.2$, 0.4 and 0.6, respectively. (b) Open circles correspond to the value of $D(\pi, \pi)$ and closed circles to D'.

with this type of the Coulomb potential in the same way as in the previous sections. It is displayed in Fig. 9, for the case of $U_0 = 8$ and ten electrons on the ladder with six rungs and two legs with the antiperiodic boundary condition along the chain. For comparison the figure also exhibits the phase diagram for the case where the long-range Coulomb interaction part is cut off for $r > 1$, which makes the interaction part identical to the n.n. Coulomb interaction with $V\ (= U_0 a/(a+1))$ for both interchain and intrachain directions. In this case with $V(r)$ in (13), the SC region is slightly enlarged. We consider it is because the tendency to the localization of electrons like Fig. 5(b) or (c) is weakened by the effect of the long-range part of the Coulomb interaction $V(r)$, since the potential difference which an electron feels when it moves from the n.n. site of another electron to the next n.n. site decreases.

This is seen in the CDW correlation functions $D(q_x, q_y)$ in Fig. 10(a), and D' in Fig. 10(b) which we have calculated in the case of $t_d = 1.05$ for various values of a. A qualitative feature of the duality relation is observed as in the previous cases; the SC features are suppressed in the state in which both the correlation functions $D(\pi, \pi)$ and D' are developed after jump-wise enhancement and the CDW correlation is dominant, similarly as in the case of the previous section. However, in the present case, both the values of $D(\pi, \pi)$ and D' grow up gradually and the jump-wise enhancement of the correlation functions is more difficult to see. Thus this type of long-range Coulomb interaction weakens the effect of the n.n. interchain and intrachain Coulomb interaction V which brings about a strong instability to a CDW state. Consequently the SC region remains alive in a slightly wider parameter space. As the result of this section the expectation for the superconductivity in a real 2C system is kept valid even if we consider the effect of the realistic long-range Coulomb interaction.

4. Summary

In this paper we have investigated the effect of the long-range part of the Coulomb interaction against the formation of the SC ground state in the 2C Hubbard model by use of the exact-diagonalization method. First, the n.n. intrachain Coulomb interaction V_p was found not to reduce the SC region appreciably, although the CDW correlation function $D(\pi, \pi)$ increased gradually due to V_p and the SC pair correlation function against the distance between pairs decayed slightly more quickly than in the simple 2C Hubbard model. An n.n. Coulomb interaction with coupling constant V working for both interchain and intrachain directions, the instability to CDW developed more rapidly and a transition from the SC state to a CDW state was observed to occur more quickly with increase of V. The SC region became narrower. However, when we included the whole part of the long-range Coulomb interaction of the type of $1/r$ in our Hamiltonian, the instability to the CDW became slightly weaker and the degree of decrease of the SC region with increase of coupling constant was not strengthened. Although the results are substantially influenced by the size effect, qualitative features of the results are considered to be correct. Therefore, we conclude that the detrimental effect of the long-range Coulomb interaction to SC in the 2C Hubbard model is not crucial. This allows the occurrence of superconductivity in real ladder materials in which the long-range Coulomb interaction is inevitable.

Acknowledgements

We thank Professor H. Tsunetsugu and Professor H. Sumi for useful advises. Parts of calculations in this paper were carried out on the DEC memory server and the IBM scalar server of the AIST RIPS Center.

References

[1] K. Yamaji, Y. Shimoi, Physica C 222 (1994) 349.
[2] J. Kondo, Prog. Theor. Phys. 29 (1963) 1.
[3] K. Yamaji, Y. Shimoi, T. Yanagisawa, Physica C 235–240 (1994) 2221.
[4] T. Yanagisawa, Y. Shimoi, K. Yamaji, Phys. Rev. B 52 (1995) R3860.
[5] A.M. Finkel'stein, A.I. Larkin, Phys. Rev. B 47 (1993) 10461.
[6] H.J. Schulz, Phys. Rev. B 53 (1996) R2959.
[7] N. Nagaosa, Solid State Commun. 94 (1995) 495.

[8] N. Nagaosa, M. Oshikawa, J. Phys. Soc. Jpn. 65 (1996) 2241.
[9] M. Kimura, Prog. Theor. Phys. 49 (1973) 697.
[10] J. Solyom, J. Low. Temp. Phys. 12 (1973) 547.
[11] A.B. Zamolodchikov, JETP Lett. 43 (1986) 730.
[12] A.B. Zamolodchikov, Sov. J. Nucl. Phys. 46 (1987) 1090.
[13] A.W.W. Ludwig, J.L. Cardy, Nucl. Phys. B 285 (1987) 687.
[14] M. Fabrizio, A. Parola, T. Tosatti, Phys. Rev. B 46 (1992) 3159.
[15] M. Fabrizio, Phys. Rev. B 48 (1993) 15838.
[16] L. Balents, M.P.A. Fisher, Phys. Rev. B 53 (1996) 12133.
[17] R.M. Noack, S.R. White, D.J. Scalapino, Physica C 270 (1996) 281.
[18] R.M. Noack et al., Phys. Rev. B 56 (1997) 7162.
[19] K. Kuroki, T. Kimura, H. Aoki, Phys. Rev. B 22 (1996) R15641.
[20] S. Koike, K. Yamaji, T. Yanagisawa, Physica C 282–287 (1997) 1765.
[21] S.R. White, Phys. Rev. Lett. 69 (1992) 2863.
[22] S.R. White, Phys. Rev. B 48 (1993) 10345.
[23] For a review, see T. Ishiguro, K. Yamaji, Organic Superconductors, Springer, Berlin, 1990.
[24] M. Uehara et al., J. Phys. Soc. Jpn. 65 (1996) 2764.
[25] S. Koike, K. Yamaji, J. Phys. Soc. Jpn. 65 (1996) 327.